JETP Letters, Vol. 79, No. 8, 2004, pp. 383–387. From Pis'ma v Zhurnal Éksperimental'noĭ i Teoreticheskoĭ Fiziki, Vol. 79, No. 8, 2004, pp. 470–474.


# Metastability and Superfluid Fraction of the A-like and B Phases of $^3$He in Aerogel in Zero Magnetic Field¶

**E. Nazaretski[1], N. Mulders[2], and J. M. Parpia[1, *]**

[1] *Laboratory of Atomic and Solid State Physics, Cornell University, Ithaca, NY 14853, USA*

[2] *Department of Physics and Astronomy, University of Delaware, Newark, DE 19716, USA*

**e-mail: jmp9@cornell.edu*

Received March 18, 2004

We report the low-frequency sound measurements of the metastable A-like (A*) phase of superfluid $^3$He confined within a 98% open aerogel matrix in zero magnetic field. The second soundlike (slow) mode provides an accurate determination of the superfluid fraction of (and the transition between) the A* and B phases. The A* and B phases exhibit stable coexistence in the presence of disorder, the ratio of their superfluid fractions ($\rho_a^{A^*}/\rho_s^B$) is much smaller than that of the bulk A and B phases, and argues that the A* and bulk A phases are distinct. © *2004 MAIK "Nauka/Interperiodica".*

PACS numbers: 67.57.Bc; 64.60.My

$^3$He is an ultrapure system that undergoes a transition from a normal Fermi liquid to the *p*-wave paired superfluid state. Strong confinement of $^3$He within regular geometries of characteristic size $\sim\xi_0$ (the superfluid $^3$He coherence length) had been predicted to significantly alter the bulk phase diagram [1], but this was never manifested in any experiments. The introduction of silica aerogel, a network of a few nm diameter $SiO_2$ strands, with fractal correlations of a few to 100 nm [2] provides a route by which superfluid $^3$He can experience correlated disorder because $\xi_0$ is larger than the strand diameter and of the same order of magnitude as the correlations.

The introduction of disorder also significantly alters the resulting phase diagram [3–6] beyond suppressing the superfluid transition temperature, $T_{ca}$. Recent work finds that a metastable A-like phase appears in both zero and finite magnetic fields, the polycritical point vanishes and the A $\longrightarrow$ B transition, $T_{AB}$ and $T_{ca}$ exhibit a width (partially attributed to temperature control and thermometry) [4, 7]. $T_{AB}$ was explored in strong magnetic fields [8]; low-field NMR results definitively identified a hysteretic A $\longleftrightarrow$ B transition at high pressure [9] and identified the equilibrium low-temperature phase of $^3$He in aerogel as the B phase [10]. However, there is controversy as to the metastability of the A-like phase in zero field [7, 11]. The only other *p*-wave paired system, the heavy fermion $UPt_3$, has a rich phase diagram that is modified by both pressure and magnetic fields [12], though the influence of disorder (other than the suppression of $T_c$) by elastic scattering [13] has yet to be mapped. Thus, there is an incomplete understanding of the effects of disorder on the phase diagrams of unconventionally paired systems.

Theoretical effort to understand the role of disorder has concentrated on the B phase [14, 15]. Only very recently, work by Fomin [16, 17], drawing on earlier general results of Volovik [18], *specifically excludes* the A phase as a stable phase in the presence of disorder and proposes other equal spin paired states as candidates for the A-like (A*) phase. However, properties that distinguish A* states from the A phase are not explicitly identified.

The A* superfluid phase that is initiated when cooling from the normal state exhibits a variety of time-dependent behavior (in magnetic fields) quite different from that of bulk A to B phase conversion. A negative frequency shift (usually associated with the $^3$He A phase) and a positive frequency shift (associated with the B phase) were observed to be simultaneously present while cooling by Barker *et al.* [9] and the Moscow group [19]. For aerogel preplated with $^4$He, the weight of A* decreased continuously over a broad temperature range [19] before abruptly vanishing below a temperature, $T_{A^*B}$ [9, 19]. The results are different without $^4$He preplating. The A* phase was unstable with a lifetime that decreased depending on the proximity to $T_{A^*B}$ [19]. Pinning [11] has been invoked to explain the finite thermal and temporal width of the A* $\longrightarrow$ B conversion process, in contrast to bulk $^3$He, where once initiated, the A $\longrightarrow$ B transition proceeds rapidly to completion.

The superfluid fraction, $\rho_s/\rho$, measured with both torsional oscillators [5, 20] and sound [21] is signifi-

¶ This article was submitted by the authors in English.

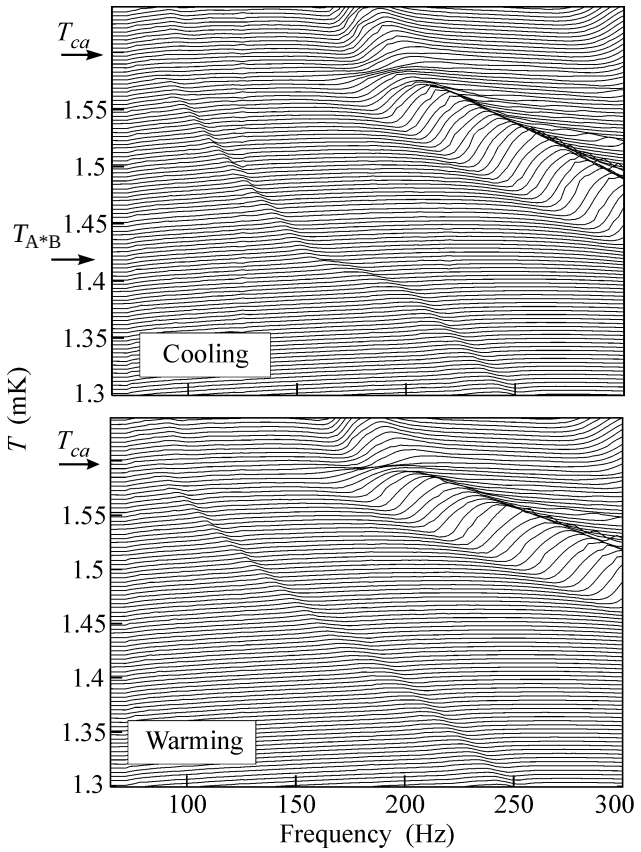


**Fig. 1.** Slow mode (SM) spectra at 21.01 bar offset vertically by temperature (the ordinate displays temperature and the received signal). The positive peak that merges into the weak "edge mode" below 100 Hz at $T_{ca}$ = 1.585 mK is the fundamental SM resonance [21]. The broad feature above 170 Hz is a Helmholtz mode combined with SM harmonics that cross close to $T_{ca}$. The upper panel shows the evolution of the SM on cooling with the A* ⟶ B transition at $T_{A*B}$ = 1.415 mK. The lower panel depicts the SM behavior on warming.

cantly suppressed from unity as $T \longrightarrow 0$. However, the A* phase superfluid density, $\rho_s^{A*}$ has not been measured to date in zero field [5, 20, 21], because data were always obtained on warming after entering the B phase (due to temperature control difficulties while cooling).

In this letter, we report on zero-field low-frequency sound measurements as a function of temperature and pressure. Zero-field results are significant because of their lack of time dependence and also because the characteristic fields that alter the phase diagram and orient textures of superfluid $^3$He can be quite small. The magnetization of the surface $^3$He that may affect the time dependence is also field-dependent. In our experiments, the stability (*no time dependence*) of the A* and B phases and mixtures of these phases against conversion to the B phase allows us to reliably evaluate $\rho_s$. The sequence of phase transitions observed during warming and cooling show the following:

(1) The A* and B phases can coexist in a long-lived metastable state.

(2) The ratio of the A* and B phase superfluid fractions $\rho_s^{A*}/\rho_s^B$ is very different from the bulk $\rho_s^A/\rho_s^B$. This ratio will be useful in establishing the nature of the A* phase.

(3) The transitions from A* to B (cooling) and B to normal (*N*) (warming) have widths of 20 and 25 μK, respectively, and could be partially penetrated to produce coexistent A* and B phases after warming from $T_{A*B}$ or cooling from $T_{ca}$. The A* phase reproducibly supercools below $T_{ca}$ before conversion to the B phase along a smooth curve $T_{A*B}$ on the *PT* diagram.

The experimental cell's cylindrical aerogel filled resonator has length $l$ = 1.64 cm and diameter $d$ = 1.27 cm. Sound is coupled to and from the $^3$He via piezoceramic wafers attached to coin silver "speaker" and "microphone" membranes that are in contact with the 98% open aerogel sample's ends [22]. The spectrum of the acoustic resonator from which the sound velocities can be obtained is determined by sweeping the excitation frequency. A susceptibility thermometer monitored the $^3$He temperature, and a $^3$He melting curve thermometer monitored the $PrNi_5$ demagnetization stage.

For a superfluid in the interstices of a compliant solid such as aerogel, the interpenetrating normal and superfluid components [23] move in phase with the aerogel to give rise to a first soundlike "fast" mode whose frequency is continuous across the superfluid transition. The onset of the "slow" mode (SM) (in which $\rho_s$ and $\rho_n$ move out of phase) analogous to fourth sound in rigid porous media or second sound in the bulk is the signature of superfluidity. These modes were first observed by McKenna *et al.* [24] for $^4$He in aerogel, and the B phase modes were mapped (on warming) in $^3$He by Golov *et al.* [21]. The SM velocity is used to determine $\rho_s/\rho$.

Examples of the SM's evolution while cooling (upper panel) and warming (lower panel) at 21.01 bar are shown in Fig. 1. The A* ⟶ B transition (width ~20 μK) is seen in the cooling trace and its onset, $T_{A*B}$, and the superfluid transition $T_{ca}$ are marked with arrows. For $T \geq T_{ca}$, the SM converts into the "edge mode" that involves counterflow of the normal fluid in the aerogel and the layer of bulk superfluid $^3$He around the aerogel [21]. Similar features were noted at all pressures between 28.6 and 13.16 bar and used to map out the phase diagram (Fig. 2).

In contrast to bulk $^3$He, where the A phase is the equilibrium high-pressure, high-temperature phase and vanishes below the polycritical point (~21 bar, see Fig. 2), our studies show no evidence for a B ⟶ A* transition (in agreement with [3, 4]). Unless the B phase

superheats (unlike the bulk), it is likely that there is no region where the A* phase is the lowest free-energy (equilibrium) phase in zero magnetic field. $T_{A^*B}$ was observed down to 13.16 bar and has marked similarities to the bulk $^3$He results of Schiffer *et al.* [25] obtained with ultraclean surfaces (Fig. 2). In traversing $T_{A^*B}$, we varied the cooling rates between 9.5 and 100 μK/h with no effect on $T_{A^*B}$ or the transition's width (~20 μK), and $T_{A^*B}$ reproduces precisely upon cycling above $T_{ca}$.

NMR features have characteristics of a combination of A and B phases [9, 19], but their coexistence cannot be studied in zero field. Brussaard *et al.* [8] showed that the A* ⟶ B transition could be arrested and reversed by altering the magnetic field. We show evidence for the metastable coexistence of the A* and B phases of $^3$He in aerogel in zero magnetic field (Fig. 3). The upper and the lower traces represent the resonant frequency in the B and A* phases, respectively. The intermediate trace was obtained by cooling into the $T_{A^*B}$ band by only ~7 μK (i.e., not traversing the transition to completion). Following this partial transition, the sample was warmed to just below the $T_{ca}$ band (defined below) and cooled while taking data. The frequency followed a path intermediate between that of the A* and B phases, implying a partial conversion from A* to the B phase. The coexistence of the A* and B phases in aerogel is evidence for strong pinning of the A*–B interface. The mixed state (without preplating with $^4$He) was stable at any temperature (including within 5 μK of $T_{A^*B}$ for a period of a day), in contrast to the Moscow group's findings [19] of instability for pure $^3$He, or a broad transition for $^4$He covered surfaces (both in a magnetic field). The stability against conversion of coexistent A* to B phases in our experiment is similar to that for the $^4$He coated case [9, 19]. This suggests that the combination of a magnetic field and the surface solid $^3$He may play a role in mediating the conversion from A* ⟶ B.

The superfluid transition, $T_{ca}$, occurs over a temperature band ~25 μK wide in accord with the heat capacity results of He *et al.* [26]. By carefully warming the sample from the B phase, we partially entered the $T_{ca}$ band. After thermal equilibration and subsequent cooling at a rate of ~40 μK/h, we observed a trace that was intermediate between the pure A* and pure B phase. Thus, if the cell was warmed to a temperature within the $T_{ca}$ band, the result was a partial conversion from the B ⟶ A* phases. We never initiated a partial or complete B ⟶ A* transition on warming unless we entered the $T_{ca}$ band which we could approach to within 2 μK (see inset to Fig. 3) [27]. The evolution of the SM was very similar to that depicted in Fig. 3, indicating that only part of the $^3$He B sample was converted back into A*. Different proportions of A* and B phase could be created depending on the depth of penetration into the $T_{ca}$ or $T_{A^*B}$ bands. The pressure-independent widths of $T_{ca}$ and $T_{A^*B}$ may be related to one another and due to inhomogeneities induced by compression of the ends of the aerogel during cell assembly. However, if the width were solely due to inhomogeneities and not pinning, we would expect the $T_{A^*B}$ width to diminish at high pressures, where the pressure dependence of $T_{A^*B}$ is weak (Fig. 2).

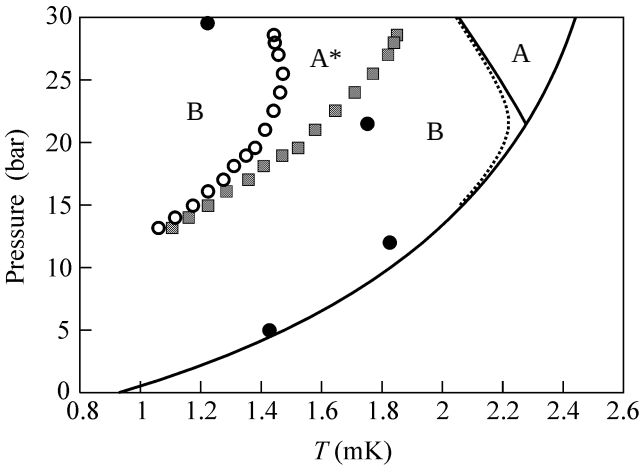


**Fig. 2.** The metastable $^3$He A* phase in 98% open aerogel in zero magnetic field is bounded by squares that mark the onset of superfluidity ($T_{ca}$) and open circles that mark the A* ⟶ B transition observed while cooling. The symbols' width is comparable to the transitions' width. Solid lines show the bulk $^3$He phase diagram in zero field, the dotted line shows the thermodynamically stable bulk B ⟶ A transition in a 24.9 mT field, and the A ⟶ B transitions observed in bulk $^3$He in a specially prepared cell (filled circles) [25]. A similar (less pronounced) $T_{A^*B}$ suppression was seen at Northwestern [3].

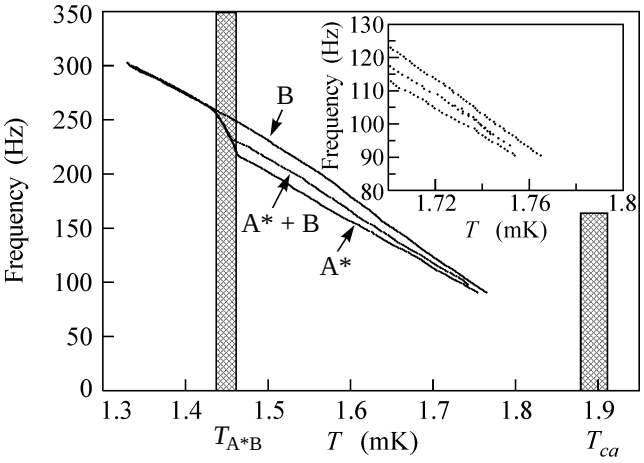


**Fig. 3.** The evolution of the peak frequency of the SM at 27.97 bar. The upper (warming) and lower (cooling) traces depict the B and A* phase results. The intermediate curve is a history-dependent trace obtained by initiating but not carrying to completion the A* ⟶ B transition. The inset shows a similar trace obtained by partial penetration into the $T_{ca}$ band. The intermediate frequency SM is evidence for the stable coexistence of the A* and B phases of $^3$He in 98% aerogel.

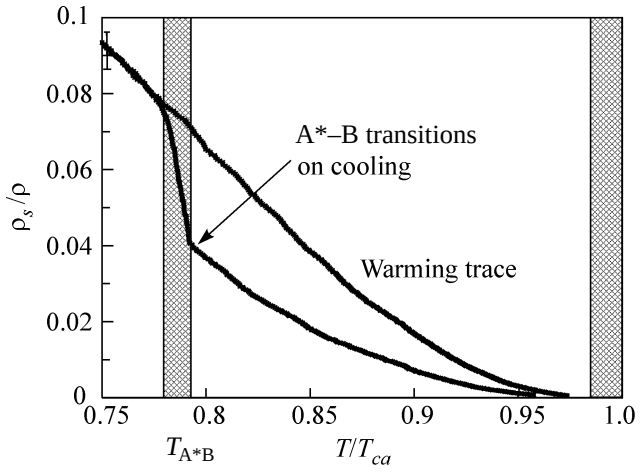


**Fig. 4.** Values of $\rho_s/\rho$ in 98% aerogel at 27.97 bar. The upper curve shows data obtained in the B phase on warming. The lower curve was recorded on cooling; both were carried out at ~40 μK/h. The lower curve shows the signature of the A* ⟶ B transition. The cooling and warming traces overlap below the $T_{A^* \to B}$ "band."

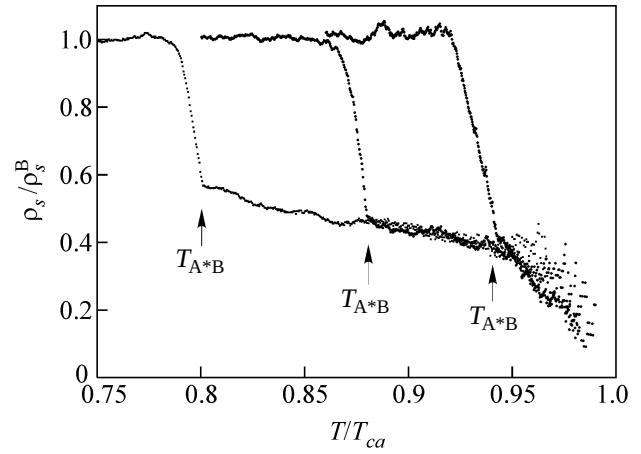


**Fig. 5.** The $\rho_s/\rho_s^B$ ratio for $P$ = 27.97, 22.53, and 16.05 bar (from left to right). Below $T_{A^*B}$ (once the transition is complete), only the B phase is present; thus, $\rho_s/\rho_s^B = 1$ ($\rho_s^B$ is a function fitted to the B phase data obtained while warming).

Analysis of the velocity of the slow mode allows us to determine the superfluid fraction through the equation $\rho_s/\rho = \rho/\rho_a(c_s/c_a)^2$, where $c_s$ is the slow mode velocity and $c_a$ is the longitudinal sound velocity in aerogel. Using this equation, we calculate the $\rho_s/\rho$ for the A* and B phases, after we subtract the frequency shift of the edge mode (described in Golov *et al.* [21]). The edge-mode velocity is $\sim(\rho_s^{bulk}/\rho)^{1/2}$ ($\rho_s^{bulk}$ is the bulk $^3$He superfluid fraction). In Fig. 4, we plot the $\rho_s/\rho$ found for the A* and B phases at 28 bar. Errors due to the extrapolation of the edge-mode frequency shift ~±1% are comparable to the scatter in the data in Fig. 4.

The B-phase superfluid fraction $\rho_s^B/\rho$ in Fig. 4 is similar to that measured by the torsional oscillator technique [5], while the supercooled A* data fall below. The superfluid density of the A* and B phases (28 bar, Fig. 4) is well fitted by the equation $\rho_s/\rho = A(1 - T/T_{ca})^b$. The (A, $b$) coefficients at 28, 22.53, and 16.05 bar are (1.2, 2.1), (1.4, 2.2), and (1.5, 3.5) and (0.83, 1.5), (1.5, 1.9), and (0.97, 2.1) for the A* and B phases, respectively. The higher exponent at 16.05 bar manifests the relatively rapid growth of $\rho_s^{A^*}$ near $T_{ca}$ seen in Fig. 5 but is confined to a limited temperature range (Fig. 2). The ratio $\rho_s^{A^*}/\rho_s^B$ diminishes near $T_{ca}$ (see Fig. 5), and the ratio $\rho_s^{A^*}/\rho_s^B \le 0.5$ is smaller than that expected for bulk $^3$He A even when **l** is oriented parallel to the superflow [28], a situation that is impractical to achieve due to wall orientation effects [29]. It is surprising that this strong suppression of $\rho_s^{A^*}$ is manifested in a medium with no preferred orientation and in the absence of a magnetic field, unless the A* phase gap is much smaller than that of the B phase.

The strong reduction of $\rho_s^{A^*}$ (and A* phase gap) compared to $\rho_s^B$ raises the following question: Why is the A* phase so reproducibly initiated from the $N$ state even in the presence of B phase within the aerogel and in the surrounding bulk fluid [4]? It is possible that the $N$ state may transform more readily into A* rather than the pseudoisotropic B phase, or the region near $T_{ca}$ may possibly contain precursor nonsuperfluid states [18, 30] that transform more readily into the A* phase.

In summary, the slow mode of $^3$He in 98% aerogel in zero field was used to quantify the A* and B phase superfluid fractions, which differ by more than a factor of two, strongly implying that the A* and bulk A phases are distinct. We mapped the metastable A* ⟶ B transition in pressure and temperature. The A* phase persists with lifetimes greater than a day well below $T_{ca}$ and can coexist on similar timescales with the B phase. We measure and quantify the width of the $T_{A^*B}$ and $T_{ca}$ transitions. It is hoped that these measurements will spur theoretical efforts to understand the effects of disorder on the phase diagram.

J.M.P. acknowledges helpful conversations with I.A. Fomin, V.V. Dmitriev, T.L. Ho, and D. Einzel. Support was provided by the NSF (grant nos. DMR-0202113 and 9970817), by the CRDF, and by NATO under SA (grant no. (PST.CLG.979379)6993/FP).

## REFERENCES


1. Y.-H. Li and T.-L. Ho, Phys. Rev. B **38**, 2362 (1988).
2. J. V. Porto and J. M. Parpia, Phys. Rev. B **59**, 14583 (1999).
3. G. Gervais, T. M. Haard, R. Nomura, *et al.*, Phys. Rev. Lett. **87**, 35701 (2001).
4. G. Gervais, K. Yawata, N. Mulders, *et al.*, Phys. Rev. B **66**, 054528 (2002).
5. J. V. Porto and J. M. Parpia, Phys. Rev. Lett. **74**, 4667 (1995).
6. D. T. Sprague, T. M. Haard, J. B. Kycia, *et al.*, Phys. Rev. Lett. **75**, 661 (1995).
7. G. Gervais, K. Yawata, and W. P. Halperin, Phys. Rev. Lett. **88**, 209602 (2002).
8. P. Brussaard, S. N. Fisher, A. M. Guenault, *et al.*, Phys. Rev. Lett. **86**, 4580 (2001).
9. B. I. Barker, Y. Lee, L. Polukhina, *et al.*, Phys. Rev. Lett. **85**, 2148 (2000).
10. H. Alles, J. J. Kaplinsky, P. S. Wootton, *et al.*, Phys. Rev. Lett. **83**, 1367 (1999).
11. S. N. Fisher, R. P. Haley, and G. R. Pickett, Phys. Rev. Lett. **88**, 209601 (2002).
12. M. Boukhny, G. L. Bullock, and B. S. Shivaram, Phys. Rev. Lett. **73**, 1707 (1994).
13. J. B. Kycia, J. I. Hong, M. J. Graf, *et al.*, Phys. Rev. B **58**, R603 (1998).
14. P. Sharma and J. A. Sauls, J. Low Temp. Phys. **125**, 115 (2001).
15. E. V. Thuneberg, S. K. Yip, M. Fogelström, and J. A. Sauls, Phys. Rev. Lett. **80**, 2861 (1998).
16. I. A. Fomin, Pis'ma Zh. Éksp. Teor. Fiz. **77**, 285 (2003) [JETP Lett. **77**, 240 (2003)].
17. I. A. Fomin, J. Low Temp. Phys. **134**, 769 (2004).
18. G. E. Volovik, Pis'ma Zh. Éksp. Teor. Fiz. **63**, 281 (1996) [JETP Lett. **63**, 301 (1996)].
19. V. V. Dmitriev, I. V. Kosarev, N. Mulders, *et al.*, Physica B (Amsterdam) **329–333**, 320 (2003).
20. K. Matsumoto, J. V. Porto, L. Pollack, *et al.*, Phys. Rev. Lett. **79**, 253 (1997).
21. A. Golov, D. A. Geller, J. M. Parpia, *et al.*, Phys. Rev. Lett. **82**, 3492 (1999).
22. E. Nazaretski, G. Lawes, D. M. Lee, *et al.*, J. Low Temp. Phys. **126**, 685 (2002).
23. L. D. Landau, J. Phys. (Moscow) **5**, 71 (1941).
24. M. J. McKenna, T. Slawecki, and J. D. Maynard, Phys. Rev. Lett. **66**, 1878 (1991).
25. P. Schiffer, M. T. O'Keefe, M. D. Hildreth, *et al.*, Phys. Rev. Lett. **69**, 120 (1992).
26. J. He, A. D. Corwin, J. M. Parpia, *et al.*, Phys. Rev. Lett. **89**, 115301 (2002).
27. The SM signal is extinguished within $0.98T/T_c$. However, if the sample is cooled after warming to within 2 μK of $T_{ca}$, we see no conversion into the A* phase.
28. S. Higashitani, J. Low Temp. Phys. **114**, 161 (1999).
29. J. E. Berthold, R. W. Giannetta, E. N. Smith, *et al.*, Phys. Rev. Lett. **37**, 1138 (1976).
30. Yu. M. Bunkov, A. S. Chen, D. J. Cousins, *et al.*, Phys. Rev. Lett. **85**, 3456 (2000).